

Properties of Bacterial Cellulose Composite Film For Flexible Substrate of Organic Light-Emitting Diode

Worakan Hosakun¹, Yanin Hosakun¹, Levente Csoka^{1*}

¹Cellulose and Biomacromolecules Research Group, University of Sopron

Corresponding Author: Worakan Hosakun

Abstract: This study mainly used dynamic mechanical analysis to investigate the dynamic mechanical response properties of films made from: bacterial cellulose (BC), bacterial cellulose/silk fibroin (S1), and two different ratios of bacterial cellulose/silk fibroin/polyvinylpyrrolidone (S2 and S3), which is intended to use as substrate for organic light emitting diodes. The average shear moduli of the films decreased in the order BC, S1, S2, S3 from 3.85 to 0.97, 0.50 and 0.09 GPa respectively in the frequency range 0.2 to 20 Hz at room temperature. The viscoelastic properties of the samples were also measured over the temperature range of -100 to 200°C at a frequency of 1 Hz. The samples of blended BC had lower values of storage modulus (G') over the whole temperature range and higher loss tangent ($\tan \delta$) values. They thus had a reduced elastic response to applied shear loads in comparison to the pure BC films. Moreover, the dried surface films were investigated by using field emission scanning electron microscope analysis. It was found that the surfaces of the dried BC films obviously present a 3-D fibril like ultrafine network. Thermal properties of the BC nanocomposite samples which are important characteristics of OLED displays were investigated by thermogravimetric differential scanning calorimetric analysis. Glass transition temperature and degradation temperature were exhibited. Sample's transparency was also studied by using UV-Visible spectroscopy.

Keywords: Dynamic mechanical analysis (DMA), Bacterial cellulose (BC), Silk fibroin (SF), Polyvinyl pyrrolidone (PVP), Mechanical properties

Date of Submission: 26-03-2019

Date of acceptance: 09-04-2019

I. Introduction

Dynamic mechanical analysis (DMA) is widely used to determine the mechanical properties of materials. Stress is applied by an oscillating force as a function of temperature or frequency which results in a corresponding strain (deformation) in the material. The ratio of stress amplitude to strain amplitude is called the complex modulus and characterizes the stiffness of the material. The complex modulus consists of the storage modulus (G'), which is the real part, and the loss modulus (G''), which is the imaginary part¹. The storage modulus represents the stiffness of a viscoelastic material and relates to the energy stored inside the material after a given force is applied. It is used for characterizing the elastic properties of a viscoelastic material. The loss modulus represents the viscous response of the material and is proportional to the energy lost as heat due to the friction between the macromolecular chains in the material. This energy cannot be recovered. The loss factor, $\tan \delta$, is defined as the ratio between G'' and G' and relates the energy lost to the recoverable energy. A high $\tan \delta$ value means that the material is inelastic and a low $\tan \delta$ value indicates that the material is more elastic². In this work, the mechanical properties of soft film samples containing bacterial cellulose fibrils (BC), silk fibroin (SF), and polyvinylpyrrolidone (PVP) as a matrix were investigated under shear loading.

Bacterial cellulose (BC) or Nata de coco is made by the *Acetobacter* species. BC has higher purity, crystallinity, porosity, water holding capacity, tensile strength and biocompatibility compared to plant cellulose because the structure of BC only contains glucose monomer and does not contain hemicellulose, lignin or pectin³. Due to its excellent properties, BC clearly has potential for future application in a number of fields, in, for example, the biomedical, electronic, food, strong paper and textile industries^{4,5}.

One of the most popular natural protein polymers for biomaterial applications is silk fibroin (SF), derived from *Bombyx mori* cocoons, owing to its outstanding biocompatibility and excellent mechanical properties⁶. *Bombyx mori* cocoons consist of two main proteins: silk fibroin and sericin proteins; the silk fibroin protein is coated with the sericin proteins. About 25–30% by weight of a silkworm's cocoon is comprised of glue-like proteins called sericins. Disulfide bonds link the light chains (molecular weight ~26 kDa) and the

heavy chains (molecular weight ~390 kDa) of the silk fibroin. Silk fibroin is a block copolymer. The core filaments are comprised of β -sheet crystal regions and semi-crystalline regions which are responsible for the silk's elasticity. In the β -sheet crystal regions, the primary structure mainly consists of the amino acid sequence (Gly-Ser-Gly-Ala-Gly-Ala)_n. Therefore, fibroin is a hydrophobic protein that forms a rigid structure and resilient materials⁶. Researchers⁷, have attempted to enhance the mechanical properties and performance of fibroin by adding or blending silk with other polymers. They studied an SF film which was reinforced by BC nanofibrils through impregnation. Also,⁸ and ⁹ reported that when SF added to BC, the surface morphology of the film became more homogenous. Much attention has been focused on these composites, since biomaterials has less environmental impacts and they can use in various fields such as biomedical area, textile, films and scaffolds, wound dressings, membranes^{9,10}.

Alternative materials of an OLED substrate include thin glass, quartz or plastic such as polyethyleneterephthalate (PET) and polyethylenenaphthalate (PEN). According to flexible display trend, it may predominate the market in several years. Glass is brittle and that is not suitable to fabricate as a flexible monitor. The promising candidates for flexible displays with great strengths are polymers. They are light in weight, inexpensive, transparent and robust¹¹. In this present work, polyvinylpyrrolidone (PVP) was used as matrix. It is a non-ionic water soluble and an amorphous polymer. It has a high glass transition temperature (T_g) due to the presence of pyrrolidone groups in the structure¹². PVP plays a significant role in the preparation of several composites and is perfectly compatible with cellulose but has poor mechanical properties¹³. These composites have been widely used in various applications e.g. electronic devices, transducers and gas sensors, owing to their unique characteristics and adaptability¹³.

Presently, the smartphones are launching the new models to replace the obsolete devices every year, raise electronic wastes (e-waste) after a few short years of the consumers use. The out-of-date electronic wastes are rapidly filling the landfill sites. In order to decrease electronic e-wastes environmentally friendly raw materials such as BC, PVP and SF were considered in the present study.

The main aim of this work is to compare the mechanical characteristics of BC/SF and BC/SF/PVP blended films with those of pure BC films for fabricating mechanically accepted substrate for transparent, lightweight, organic, light emitting diodes (OLED) substrate application. The shear modulus and dynamic mechanical characteristics were investigated using the DMA technique first time on self-standing nano and microfibrillated BC film and on its composite. Moreover, the surface of dried films, thermal properties and transparency were presented.

II. Material And Methods

Purification of BC

The Nata de coco (coconut gel) was kindly supplied by Mr. and Mrs. Tongampai's production, Thailand. It was first cut into small cubes and soaked in water for several days until a pH of ~6 was reached. Then, the nata de coco was boiled in distilled water until the pH reached ~7. Afterwards, the material was given a 0.01 M NaOH solution treatment at 80°C under continuous stirring to remove any remaining microorganisms and medium components, following the method of ¹⁴. After alkaline treatment, the colour of the nata de coco lost its original yellow colour and turned into a pale white/transparent gel. The clear gel was boiled in distilled water several times until the pH of the water became neutral. Finally, the purified nata de coco was blended in a laboratory blender and poured into silicone trays before it was dried in an oven at 32°C.

Preparation of microfibrillated BC

After the BC film was completely dry, 0.08 g of the material was cut into small pieces and immersed in 80 ml distilled water to obtain a 0.1% w/v suspension. It was then subjected to ultrasonication at a low frequency (20 kHz) using an ultrasonic horn (Tesla 150 WS) with a tip diameter of 18 mm, until a well-dispersed colloid was achieved.

Preparation of nanocrystalline BC

In order to obtain nanocrystalline BC, dried BC films (0.08g) were placed in a desiccator for 3 days with a 37% HCl fuming solution. Due to the vapour phase of the HCl, degradation of the amorphous part of cellulose occurred and nanocrystalline BC was obtained¹⁵. This was subsequently immersed in 80 ml distilled water and subjected to ultrasonication following the same method as was used in preparing the microfibrillated BC.

Purification of silk cocoons (degumming)

Bombyx mori silk cocoons were boiled in 0.02 M Na₂CO₃ for 30 minutes and washed twice in 50°C water. Afterwards, the degummed silk fibroin was dried in an oven at 70°C. Once the degumming step was complete, the dried silk fibroin (0.32 g) was placed in a desiccator for 2 days with a 37% HCl fuming solution in

order to obtain nanosilk. Thereafter, the silk fibroin was easily dispersed in distilled water (80 ml) using ultrasonication.

Preparation of PVP solution and composite films

To obtain PVP solution, PVP powder was dissolved in methanol. The PVP solution was then poured into the BC and SF solutions before the resulting mixtures were dried in an oven. Table 1 shows the compositions of the different solutions prepared.

Table no 1:The percentage of each component in the solutions used for the preparation of samples (%)

Sample No.	Microfibrillated BC (%)	Nanocrystal BC (%)	Nanocrystal SF (%)	PVP (%)
BC control	66.67	33.33	-	-
S1	28.57	14.29	57.14	-
S2	10.26	5.13	20.51	64.10
S3	6.25	3.13	12.50	78.13

Dynamic mechanical analysis (DMA)

Dynamic mechanical analysis (DMA) was used to measure the viscoelastic properties of the nanocomposite films as a function of temperature and frequency. The testing equipment used was a METRA VIB DMA 50 with the DYNATEST 6.9 software. The DMA was undertaken in shear mode and the starting strain was 0.001. The shear storage modulus (G') and energy dissipation factor ($\tan \delta$) were measured during a frequency sweep and temperature sweep. In the case of the frequency sweep, the frequency of the loading was varied from 0.2 Hz to 20 Hz at room T; for the temperature sweep, the temperature was increased from -100°C to 200°C with a heating rate of 3°C/min at a loading frequency of 1 Hz.

Field Emission Scanning Electron Microscope (FE-SEM)

FE-SEM micrographs of substrate sample (BC control and S2) were obtained from TescanOrsayHolding, a.s., Czech Republic by using the high-resolution field emission microscope FE-SEM (Tescan MIRA3 FE-SEM). FE-SEM was used for investigating the substrate’s morphology. Samples were observed at low acceleration voltage of 3 kV. The sample was attached on aluminum sample holders and coated with 4 nm of ultrafine Pt in order to eliminate the charging of the samples before testing.

Thermogravimetric differential scanning calorimetric analysis (TG-DSC)

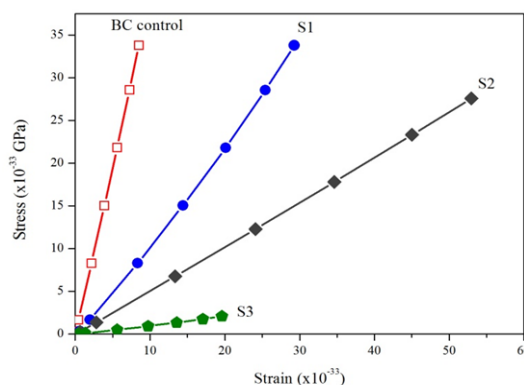
Thermograms of BC nanocomposite samples were obtained from a Perkin Elmer Diamond thermogravimetric-differential scanning calorimeter (TG-DSC). The experiment was performed from ambient temperature up to the maximum temperature of 500°C at the constant heating rate of 2°C/min in nitrogen atmosphere.

Ultraviolet-visible (UV-VIS) spectroscopy

Ultraviolet-visible (UV-Vis) spectra were investigated on WPA lightwave S2000 UV/VIS spectrophotometer for recording the light transmittance of the samples over the visible wavelength. A base line was recorded and calibrated using air.

III. Result

Shear modulus, denoted by G , is the ratio of shear stress (σ) to shear strain (ϵ) was obtained from DMA testing. The stress–strain curves for the BC control, S1, S2, and S3 samples are shown in Fig. 1.



Figureno 1: Stress–strain curves of BC control, S1, S2, and S3

It can be seen that the value of G for the BC control sample (~3.85 GPa) was greater than those of S1, S2, and S3 samples, summarized in Table 2.

Table no 1: Average shear modulus and shear storage modulus of BC control, S1, S2 and S3 at frequency ranges from 0.2 to 20 Hz.

Sample	Average shear modulus (GPa)	Average shear storage modulus (GPa)
BC control	3.85	3.78
S1	0.97	0.85
S2	0.50	0.48
S3	0.09	0.08

Therefore, BC has the highest resistance to shear loading. This is because the BC control material has a more compact structure than the other materials. The second highest G value was for the S1 sample, for which the average value of G was 0.97 GPa. S1 contained SF which made the film brittle and reduced the stiffness of the material but at the same time the corresponding strain increased significantly. Due to the fact that, the presence of SF in BC film could improve the strength of the film by the strong interactions between them and increase β -sheet structure but in this situation the ratio of BC and SF was insufficient proportions. The G values for S2 and S3 were 0.50 and 0.09 GPa respectively and strain value for S3 was the highest between the composites. The lower stiffnesses of S2 and S3 under shear loading may have been caused by the rigid group in the PVP chain.

In this work, DMA was performed to study the dynamic mechanical behaviour of the BC control, S1, S2 and S3 films. The mechanical properties tested included the elasticity and viscosity.

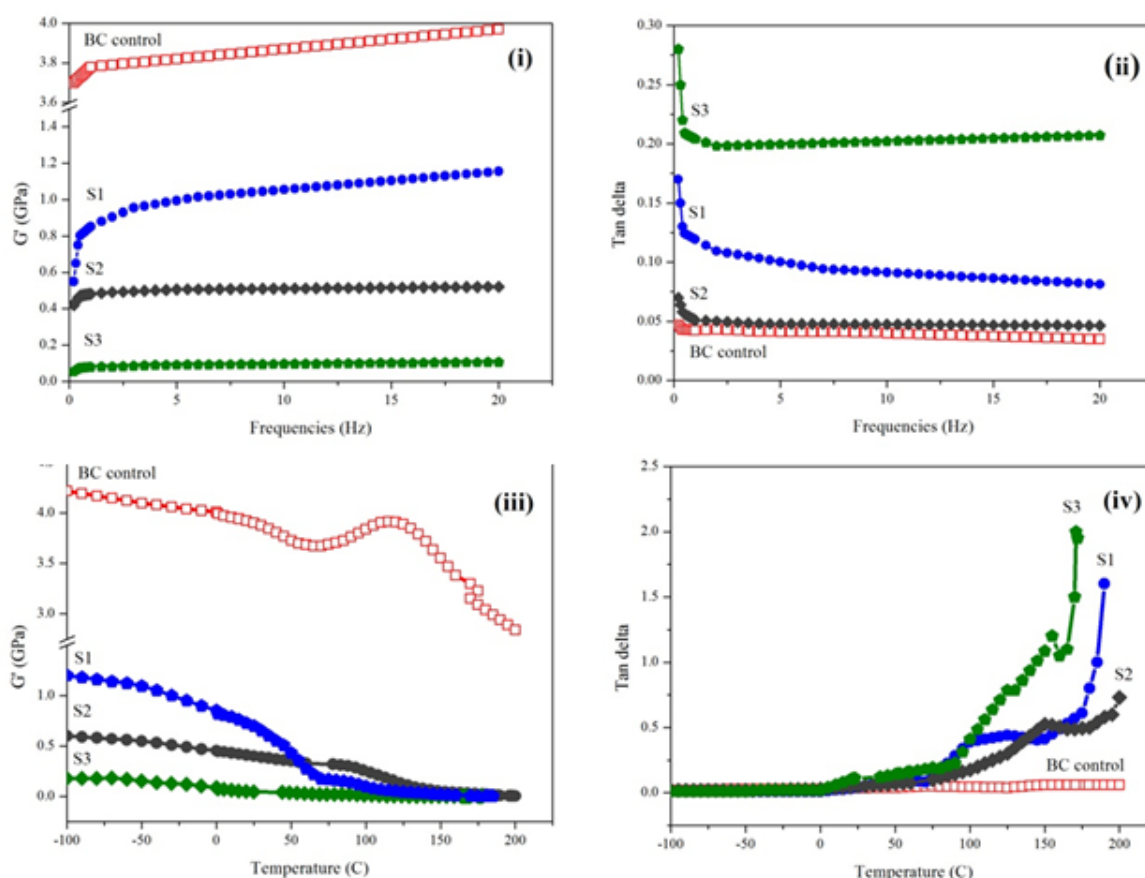


Figure no 2: Storage modulus (G') and dynamic loss tangent ($\tan \delta$) at different frequencies (i,ii), and at different temperatures (iii,iv) of BC control, S1, S2, and S3.

Figure 2(i) shows the shear storage modulus results for tests carried out at different frequencies (0.2 to 20 Hz) at room temperature. The measured values of G' are shown in Table 2.

It was found that the shear storage modulus (G') values of the BC control sample shows the highest due to the three-dimensional network structure of BC as confirmed by FE-SEM result. The G' values for S1, S2, and S3

increase slightly for frequencies from 0.2 to 20 Hz. As can be seen from the data, S1 has a lower strength than BC control due to the brittle characteristics of SF. Liang and Hirabayashi¹⁶ prepared silk fibroin-alginate blend films and found that strong hydrogen bonding interactions encourage β -sheet conformation of silk fibroin formation. The optimal BC/SF ratio was found by these authors to be 75:25, producing the strongest intermolecular interactions. A lower ratio results a rigid film and the structure of the silk fibroin protein changes and reduces the ability of the film to react elastically to an applied force. In terms of S2 and S3, SF and PVP were studied for compatibility with BC. The amount of PVP seems to affect the mechanical properties of these samples. Going, Sameoto, and Ayranci¹⁷ found that after 10% wt of cellulose nanocrystals were loading to PVP polymer, the elastic modulus and strain values were dropped, which might be due to the fact that the crack occurrence after cellulose nanocrystals addition generates stress concentration.

Data for the dynamic loss tangent ($\tan \delta$) are shown in Fig 2(ii) for the range of frequencies tested. As mentioned previously, $\tan \delta$ is the ratio of loss modulus (G'') to the storage modulus (G'). It can be used to explain the movement of the polymer chain molecules and changes in the structure¹⁸. As can be seen from the results, all of the $\tan \delta$ curves decrease significantly up to frequencies of ~ 1 Hz and then remain flat as the frequency continues to increase. As can be seen from the curves, BC control had the lowest values of $\tan \delta$. Looking at the data in fig 2(iii) and (iv), the glass transition temperature can be clearly observed by the decreases in G' and the peaks in $\tan \delta$. The G' value of BC control decreased as the temperature was increased from -100°C to 200°C . The storage modulus was about 4.2 GPa at -100°C and gradually decreased to 2.75 GPa at 200°C with a peak in $\tan \delta$ at around 70°C defining its glass transition temperature (T_g). The appeared peak of $\tan \delta$ at about 130°C is associated with the weak hydrogen bonds rupture¹⁹. The G' value for S1 dropped significantly and was much lower than the G' value of BC control at all temperatures. It decreased from 1.25 to 0.5 GPa before the material reached its T_g ($\sim 50^\circ\text{C}$) when there was a notable decrease. The $\tan \delta$ peak occurred at 120°C which corresponds with the T_g of silk fibroin. This response is due to important intermolecular interactions between natural polysaccharides and the SF protein, which occurred after the blending, mixing or coating to make the composites. These interactions consist of hydrogen bonding, electrostatic interactions, and covalent bonding⁹. In the case of the PVP composite films (S2 and S3), the G' values began decreasing gradually at 150°C and 80°C , respectively as the films entered their glass transition. In contrast, the $\tan \delta$ values of both samples increased at these temperatures. This means that blending PVP with the films decreases the elastic characteristics of the material. This is probably because the PVP has rigid groups like five-membered rings in its structure which stiffen its backbone.

Morphology of dried BC and BC-SF-PVP (S2) samples were analyzed by using FE-SEM are depicted in Figure 3(i) and (ii).

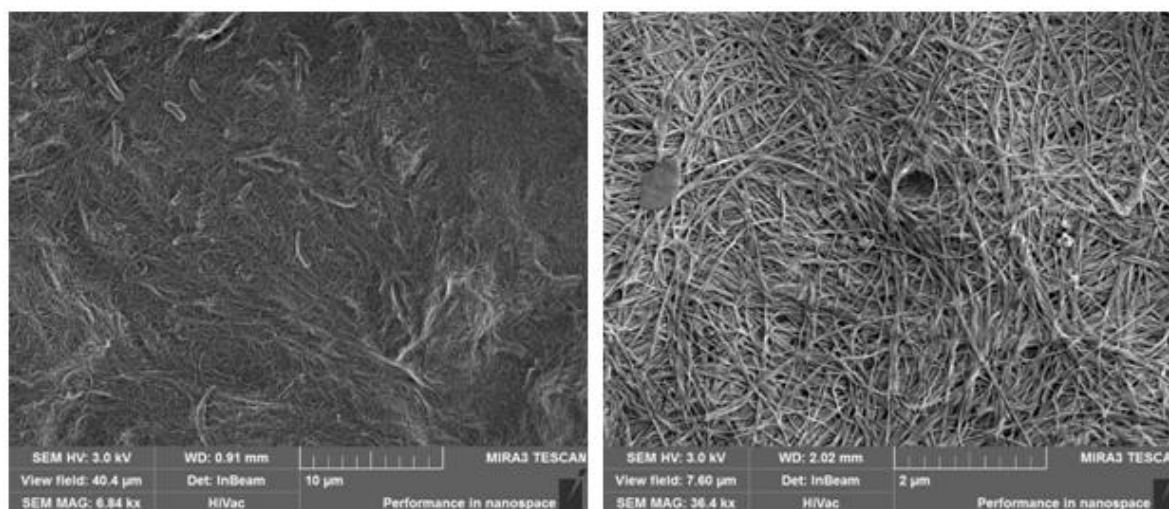


Figure no 3: FE-SEM micrograph of pure BC (i) and BC-SF-PVP (ii) dried substrates

The surface of this dried BC films obviously presents a 3-D fibrous ultrafine network structure. It can be observed that the OLED's substrate surface smoothness was increased after adding polyvinylpyrrolidone matrix, where the silk and bacterial cellulose nanofibrils has been embedded as clearly observed in Figure 3(ii). Uniformly embedded BC fibrils in the substrate demonstrate strong interaction between the BC fibrils and PVP matrix.

Thermogravimetric-differential scanning calorimetry (TG-DSC), which is a technique for analysing thermal properties of material were investigated as presented in Figure 4(i) and (ii).

According to Figure 4(i), at temperature before 100°C is corresponding to water evaporation. In the case of glass transition (T_g) temperature, the endothermic peaks at 162.8 and 165°C were found for S2 and S3 samples, respectively, which corresponds to PVP matrix²⁰. Therefore, the content of PVP causes the increasing of T_g due to the more condense and rigid structure. Moreover, BC did not affect to the T_g of the PVP matrix. Degradation temperatures of both dried films were conducted as evident from the curves shown in Figure 4(ii). S2 sample presented the degradation temperature of 408.4°C while the S3 film had the higher degradation temperature of 409.7°C. In case of BC dried film, it exhibited the degradation temperature at 370°C, hence, the embedded of PVP matrix to the BC nanocomposite film led to an increasing of thermal decomposition temperature¹⁴.

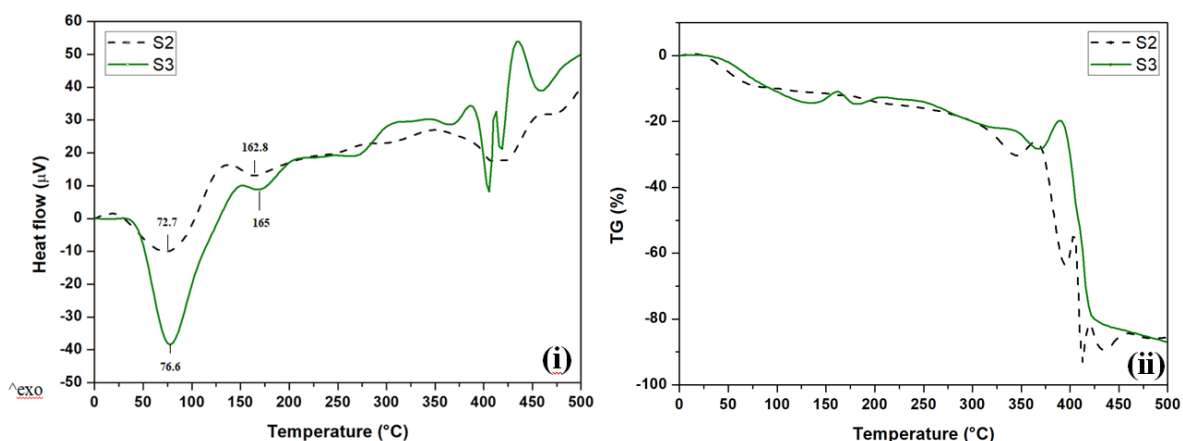


Figure no 4: DSC (i) and TG (ii) curves of S2 (dash line) and S3 (solid line) dried films at a heating rate of 2°C/min

In the case of sample transparency (Figure 5), BC-SF-PVP films exhibited ~55% of the optical transmittance at 550 nm whereas BC control and BC-SF films presented lower than 2% which was measured by Ultraviolet-visible (UV-VIS) spectroscopy. However, BC-SF-PVP films are still maintained at a favourable level for OLED screen.

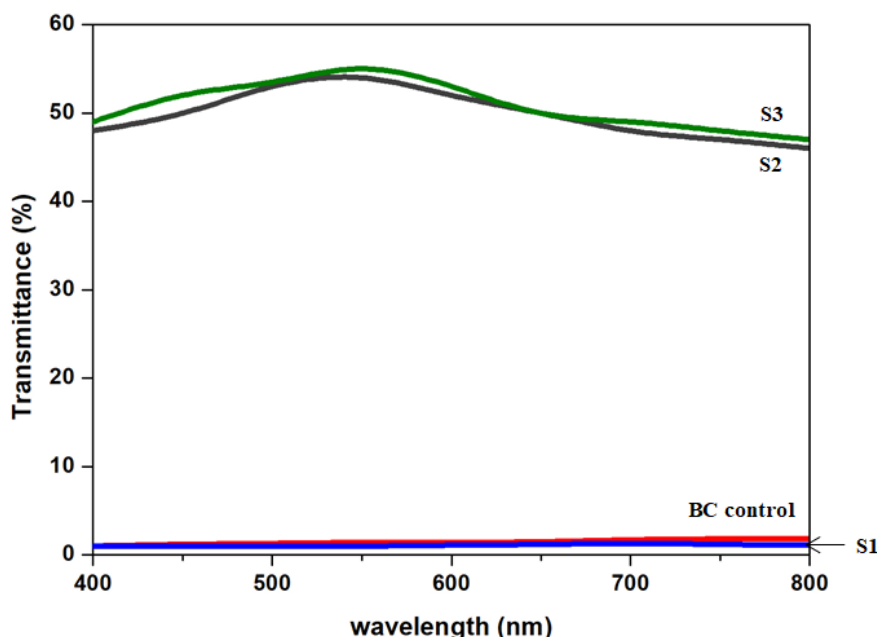


Figure no 5: Light transmittance of BC control and BC nanocomposite films at visible wavelength

IV. Conclusion

In this work, biodegradable materials were selected as a candidate to reduce e-wastes. DMA was used successfully to investigate the effect of SF and PVP on the mechanical properties and viscoelastic behaviour of BC blended OLED substrate films. According to the results obtained, the shear moduli of the composite films were clearly lower than that of the pure BC film. Moreover, the shear storage modulus and tan delta values were discussed. The BC film showed a greater stiffness than the other samples because its structure consists of a fine web-like network. Intermolecular bonding between BC and SF resulted in a rigid film because of the lower proportion of cellulose. Furthermore, the higher content of PVP matrix also caused a decrease in the mechanical properties of the composite film. Therefore, both films containing PVP had the lowest stiffness of all the samples. The surface smoothness increased after BC incorporation of PVP matrix. Moreover, it was thermally stable up to 400°C which is good for OLED applications.

V. Summary

This study used dynamic mechanical analysis (DMA) to investigate the dynamic mechanical response properties of films made from: bacterial cellulose (BC), bacterial cellulose/silk fibroin (S1), and two different ratios of bacterial cellulose/silk fibroin/polyvinylpyrrolidone (S2 and S3), which is intended to use as substrate for organic light emitting diodes. The average shear moduli of the films decreased in the order BC, S1, S2, S3 from 3.85 to 0.97, 0.50 and 0.09 GPa respectively in the frequency range 0.2 to 20 Hz at room temperature. The viscoelastic properties of the samples were also measured over the temperature range of -100 to 200°C at a frequency of 1 Hz. The samples of blended BC had lower values of storage modulus (G') over the whole temperature range and higher loss tangent ($\tan \delta$) values. They thus had a reduced elastic response to applied shear loads in comparison to the pure BC films. Some investigation of dried surface samples and glass transition temperature were explained. The surface of pure BC dried film obviously presents a 3-D fibrous ultrafine network structure and the BC nanocomposite substrate surface smoothness was increased after adding polyvinylpyrrolidone matrix, where the silk and bacterial cellulose nanofibrils has been embedded. The glass transition temperature and degradation temperature of S2 and S3 were presented. It was observed that the content of PVP causes the increasing of both T_g and thermal degradation temperature due to the more condense and rigid structure.

Acknowledgement

The authors would like to acknowledge the Human Resource Development Programme (HRDOP 3.6.1-16-2016-00018) "Improving the role of research+development+innovation in the higher education through institutional developments assisting intelligent specialization in Sopron and Szombathely" at University of West Hungary as well as part of the project GINOP-2.3.3-15-2016-00038, "Further processing of wood and wood products based on green chemistry and technology, through creating modern research infrastructure" in the framework of the Széchenyi2020 Programme. The implementation of this project is supported by the European Union, co-financed by the European Regional Development Fund.

References

- [1]. Dynamic Mechanical Analysis in the Analysis of Polymers and Rubbers. Encyclopedia of Polymer Science and Technology
- [2]. Rat S, Nagy V, Suleimanov I, Molnar G, Salmon L, Demont P, Csóka L, Bousseksou A Elastic coupling between spin-crossover particles and cellulose fibers. *Chemical Communications*, 2016;52(75):11267-11269.
- [3]. Dayal MS, Catchmark JM Mechanical and structural property analysis of bacterial cellulose composites. *Carbohydrate Polymers*, 2016;144:447-453.
- [4]. Esa F, Tasirin SM, Rahman NA Overview of Bacterial Cellulose Production and Application. *Agriculture and Agricultural Science Procedia*, 2014;2:113-119.
- [5]. Wan YZ, Hong L, Jia SR, Huang Y, Zhu Y, Wang YL, Jiang HJ Synthesis and characterization of hydroxyapatite-bacterial cellulose nanocomposites. *Composites Science and Technology*, 2006;66(11-12):1825-1832.
- [6]. Rockwood DN, Preda RC, Yucel T, Wang X, Lovett ML, Kaplan DL Materials fabrication from Bombyx mori silk fibroin. *Nat. Protocols*, 2011;6(10):1612-1631.
- [7]. Choi Y, Cho SY, Heo S, Jin HJ Enhanced mechanical properties of silk fibroin-based composite plates for fractured bone healing. *Fibers and Polymers*, 2013;14(2):266-270.
- [8]. Freddi G, Romanò M, Massafra MR, Tsukada M Silk fibroin/cellulose blend films: Preparation, structure, and physical properties. *Journal of Applied Polymer Science*, 1995;56(12):1537-1545.
- [9]. Shang S, Zhu L, Fan J Intermolecular interactions between natural polysaccharides and silk fibroin protein. *Carbohydrate Polymers*, 2013;93(2):561-573.
- [10]. Li WY, Jin AX, Liu CF, Sun RC, Zhang AP, Kennedy JF Homogeneous modification of cellulose with succinic anhydride in ionic liquid using 4-dimethylaminopyridine as a catalyst. *Carbohydrate Polymers*, 2009;78(3): 389-395.
- [11]. Acharya C, Ghosh SK, Kundu SC Silk fibroin protein from mulberry and non-mulberry silkworms: cytotoxicity, biocompatibility and kinetics of L929 murine fibroblast adhesion. *Journal of Materials Science: Materials in Medicine*, 2008;19(8):2827-2836.
- [12]. Rajeswari N, Selvasekarapandian S, Karthikeyan S, Sanjeeviraja C, Iwai Y, Kawamura J Structural, vibrational, thermal, and electrical properties of PVA/PVP biodegradable polymer blend electrolyte with CH₃COONH₄. *Ionics*, 2013;19(8):1105-1113.
- [13]. Khalil AM, Hassan ML, Ward AA Novel nanofibrillated cellulose/polyvinylpyrrolidone/silver nanoparticles films with electrical conductivity properties. *Carbohydrate Polymers*, 2017;157:503-511.

- [14]. Ummartyotin S, Juntaro J, Sain M, Manuspiya H Development of transparent bacterial cellulose nanocomposite film as substrate for flexible organic light emitting diode (OLED) display. *Industrial Crops and Products*, 2012;35(1):92-97.
- [15]. Kontturi E, Meriluoto A, Penttilä P, Serimaa R 241st ACS National meeting and Exposition: Chemistry of Natural Resources, Anaheim, CA, USA March 27-31, 2011.
- [16]. Liang CX, Hirabayashi K Improvements of the physical properties of fibroin membranes with sodium alginate. *Journal of Applied Polymer Science*, 1992;45(11):1937-1943.
- [17]. Going RJ, Sameoto DE, Ayranci C Cellulose Nanocrystals: Dispersion in Co-Solvent Systems and Effects on Electrospun Polyvinylpyrrolidone Fiber Mats. *Journal of Engineered Fibers and Fabrics*, 2015;10(3):155-163.
- [18]. Yuan Q, Yao J, Huang L, Chen X, Shao Z Correlation between structural and dynamic mechanical transitions of regenerated silk fibroin. *Polymer*, 2010;51(26):6278-6283.
- [19]. Yano S, Maeda H, Nakajima M, Hagiwara T, Sawaguchi T Preparation and mechanical properties of bacterial cellulose nanocomposites loaded with silica nanoparticles. *Cellulose*, 2008;15(1):111-120.
- [20]. Jadhav N, Gaikwad DV, Nair K, Kadam H Glass transition temperature: Basics and application in pharmaceutical sector. *J. Pharm.* 2009;3(2):82-89.

Worakan Hosakun. "Properties of Bacterial Cellulose Composite Film For Flexible Substrate of Organic Light-Emitting Diode." *IOSR Journal of Polymer and Textile Engineering (IOSR-JPTE)* , vol. 6, no. 2, 2019, pp. 42-49.